Journal of Zhejiang University-SCIENCE A (Applied Physics & Engineering) *2023 24(11):991-1002*
www.jzus.zju.edu.cn; www.springer.com/journal/11582
E-mail: jzus_a@zju.edu.cn

Research Article

https://doi.org/10.1631/jzus.A2200551

Experimental and theoretical analysis of a hybrid vibration energy harvester with integrated piezoelectric and electromagnetic interaction

Shifan HUANG, Weihao LUO, Zongming ZHU, Zhenlong XU, Ban WANG, Maoying ZHOU✉, Huawei QIN

School of Mechanical Engineering, Hangzhou Dianzi University, Hangzhou 310018, China

Abstract: Harvesting vibration energy has attracted the attention of researchers in recent decades as a promising approach for powering wireless sensor networks. The hybridization of piezoelectricity and electromagnetism has proven helpful in the improvement of vibration energy harvesting. In this study, we explore the integration of piezoelectric and electromagnetic parts in one vibration energy harvesting device. Lumped-parameter models of the system are derived considering the different connection topologies of the piezoelectric and electromagnetic parts. Numerical predictions from these models are compared with experimental results to throw light on the nonlinearities in the system. Modifications of the system are also explored to provide insights into opportunities to improve its performance and that of future vibration energy harvesters.

Key words: Hybrid energy harvesting; Nonlinear interaction; Magnetic spring; Piezoelectricity; Electromagnetism

1 Introduction

Recent years have witnessed the rapid development of wireless sensor networks and their vast applications in consumer electronics, industrial automation, and environmental monitoring (Kandris et al., 2020; Malik et al., 2020; Priyadarshi et al., 2020). In this process, a major concern has been the power supply of such networks, which currently relies on batteries and suffers from a high cost of maintenance (Priyadarshi et al., 2020). In view of the ubiquitous presence of vibration in the ambient environment, it is feasible in principle to harness available vibration energy and convert it into electricity for sensors. The so-called vibration energy harvester has emerged from this idea and has attracted the attention of numerous researchers (Zhou et al., 2018; Malik et al., 2020; Miller et al., 2020; Yao et al., 2023). According to their underlying mechanisms of energy transduction, several sorts of vibration energy harvesters are found in the literature: electrostatic energy harvesters (Basset et al., 2014; Zhang et al., 2016, 2018), triboelectric energy harvesters (Zhu et al., 2013; Li et al., 2015; Qiu et al., 2020), electromagnetic energy harvesters (Zhang et al., 2015; Saravia, 2019; Shi et al., 2020; Wang W et al., 2022), and piezoelectric energy harvesters (Cao et al., 2015; Zhang and Qin, 2019; Wang ZM et al., 2022; Wu and Xu, 2022). Among these, piezoelectric vibration energy harvesters (PVEHs) have shown superior potential for application due to their high voltage output and simple structure.

Physically, PVEHs operate in resonant mode to achieve high efficiency of energy conversion (Anton and Sodano, 2007; Safaei et al., 2019). One problem with these PVEHs has been their limited working frequency bandwidth. Great efforts have been made to enlarge the bandwidth of PVEHs, including the automatic tuning of their resonant frequencies (Challa et al., 2011), integration of multiple PVEHs with different resonant frequencies (Dechant et al., 2017), combination of PVEHs with other energy transduction mechanisms (Fan et al., 2018c; Liu et al., 2021), and intentional introduction of nonlinearity into PVEHs (Zou et al., 2017; Fan et al., 2018b). Of practical interest here is the combination of piezoelectric and electromagnetic energy harvesters. On the one hand, the frequency

✉ Maoying ZHOU, myzhou@hdu.edu.cn
Maoying ZHOU, https://orcid.org/0000-0002-0306-7863

Received Nov. 20, 2022; Revision accepted Jan. 6, 2022;
Crosschecked June 21, 2023; Online first Aug. 1, 2023

bandwidth is broadened due to the different resonant frequencies of piezoelectric and vibration electromagnetic energy harvesters. On the other hand, introduction of magnetic interaction provides an opportunity to further increase the frequency bandwidth with the help of nonlinearity.

Hence, many researchers have tried to construct and investigate hybrid energy harvesters based on piezoelectricity and electromagnetism (HEHPEs) (Xia et al., 2015; Ahmad and Khan, 2021). Magnetic interactions between permanent magnets and conducting coils have been introduced to conventional piezoelectric energy harvesters (Challa et al., 2009). Under the action of base excitation, the piezoelectric beam undergoes elastic vibration. As a result, the permanent magnets oscillate relative to the conducting coil. Electrical output can then be expected from the coil according to the principles of electromagnetism. Different arrangements between the magnets and the coils have been explored, based on spiral coils (Yang et al., 2010; Zhang et al., 2019) or helical coils (Sang et al., 2012; Xu et al., 2017b). Magnetic springs formed by the nonlinear interactions between different magnets have also been used to connect the piezoelectric and electromagnetic parts of the HEHPEs (Xu et al., 2016; Xia et al., 2017). The optimal operation frequency of the HEHPE can be easily tuned by the nonlinear magnetic spring introduced. An interesting approach to integrate the piezoelectric and electromagnetic parts in an HEHPE is to add an electromagnetic energy harvesting unit to the free end of a piezoelectric energy harvesting unit (Shan et al., 2013; Mahmoudi et al., 2014; Li et al., 2016; Liu et al., 2019). In this case, a multi-degree of freedom (DOF) vibration system is formed, increasing the power output of the hybrid system. Other investigations have focused on the introduction of impact or contact to tune the operation frequency of HEHPEs (Fan et al., 2018a, 2018b; Halim et al., 2019; Maamer et al., 2019; Iqbal et al., 2021). Nonetheless, it seems that the full potential of HEHPEs has not yet been revealed. Due to the mismatching characteristics of stand-alone piezoelectric and electromagnetic energy harvesters (Arroyo et al., 2012), nearly all the proposed and investigated HEHPEs disconnect the output of the piezoelectric part from that of the electromagnetic part. Hence, the outputs of these two parts are considered and evaluated separately. Meanwhile, due to the capacitive property of a piezoelectric energy harvester, addition of an external inductor alters the vibration characteristics of the device (Wang B et al., 2022). Noting that coils are typical electrical inductors, the electrical connection between the piezoelectric and electromagnetic parts inside an HEHPE may also alter and enhance the performance of an HEHPE (Huang et al., 2022).

In this study, we investigated the direct integration of piezoelectric and electromagnetic energy harvesting units in one HEHPE. An electromagnetic part based on magnetic springs was attached to the free end of a piezoelectric part in an HEHPE. Lumped-parameter models of the HEHPE were established considering different connection topologies between the piezoelectric and electromagnetic parts. Experimental results were obtained and compared with theoretical predictions considering the nonlinearities in the HEHPE. Modifications of the HEHPE were also explored to provide insights into the potential to improve the performance of HEHPEs and that of future vibration energy harvesters.

2 Structure and working principle

Nonlinearity added to a vibration energy harvester enlarges the bandwidth of the originally linear system (Tran et al., 2018). The HEHPE discussed in this study is similar to that described by Shan et al. (2013) (Fig. 1). It consists of a piezoelectric part, an electromagnetic part, and electrical connections. The piezoelectric part is composed of a piezoelectric cantilever bimorph beam. The bimorph beam comprises two piezoelectric plates and a base plate. The two piezoelectric plates are polarized in the same direction (as shown in the lower corner

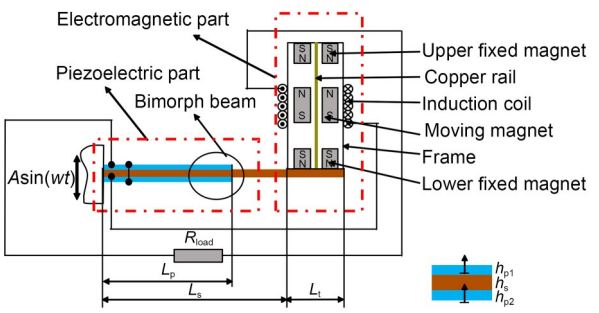

Fig. 1 Schematic diagram of the studied HEHPE. L_p and L_s are the lengths of the piezoelectric plates and base beam, respectively, and L_t is the extended length of the piezoelectric plates

of Fig. 1). The electromagnetic part is formed by two fixed ring magnets at the upper and lower ends respectively, a magnet in the middle moving along a copper rail guide, an induction coil, and a tubular frame. The whole electromagnetic part is attached to the free end of the piezoelectric part as an attached mass. Magnetic poles of the moving and fixed magnets are arranged in such a way that the forces between the moving magnet and the upper and lower fixed magnets are both repulsive. At first, the fixed magnet is kept in a balanced position under the action of these two repulsive forces. Gravity is omitted here due to its smallness compared to the magnetic repulsive forces. To avoid asymmetric wobbling of the moving magnet, a thin copper rail is set in the axis of the tubular frame to guide the motion of the moving magnet (Fig. 1). In Fig. 1, $A\sin(wt)$ is the excitation acceleration with A being the amplitude, w being the angular frequency, and t being the time. h_{p1}, h_{p2}, and h_s are the thicknesses of the top piezoelectric plates, lower piezoelectric plates, and base beam, respectively.

In the case of external base excitation of a sinusoidal waveform, the piezoelectric cantilever beam is set into continuous vibration, and the free end undergoes periodical vibration of a certain waveform. As a result, the magnetic part is forced into nonlinear vibrations. When the piezoelectric plates and the induction coil are connected to certain external electrical elements, electrical output is expected, and the so-called energy harvesting is achieved. A salient feature that differentiates this study from that of Shan et al. (2013) is that several different topologies of the electrical connections between the electromagnetic and the piezoelectric parts in the devices are considered. In Fig. 1, the piezoelectric and electromagnetic parts are electrically connected in series, and then to an external resistance load R_{load}. More details of the connection topologies are given in Section 3.

3 Theoretical model of the HEHPE

3.1 Lumped-parameter representation of the system

As indicated above, the dynamic behavior of the HEHPE is affected by the connection topology between the electromagnetic and piezoelectric parts. Four connection topologies were considered: connection topology 1, connection topology 2, connection topology 3, and connection topology 4.

Connection topology 1 (Fig. 2a) acted as a control. There is no moving magnet in the electromagnetic part and the induction coil is not connected to electrical elements. An external load resistance R_p is connected to the piezoelectric part. Connection topology 2 (Fig. 2b) differed from connection topology 1 in which the moving magnet is retained, but the induction coil is still not connected to any external electrical element. In connection topology 3 (Fig. 2c), an extra load resistance

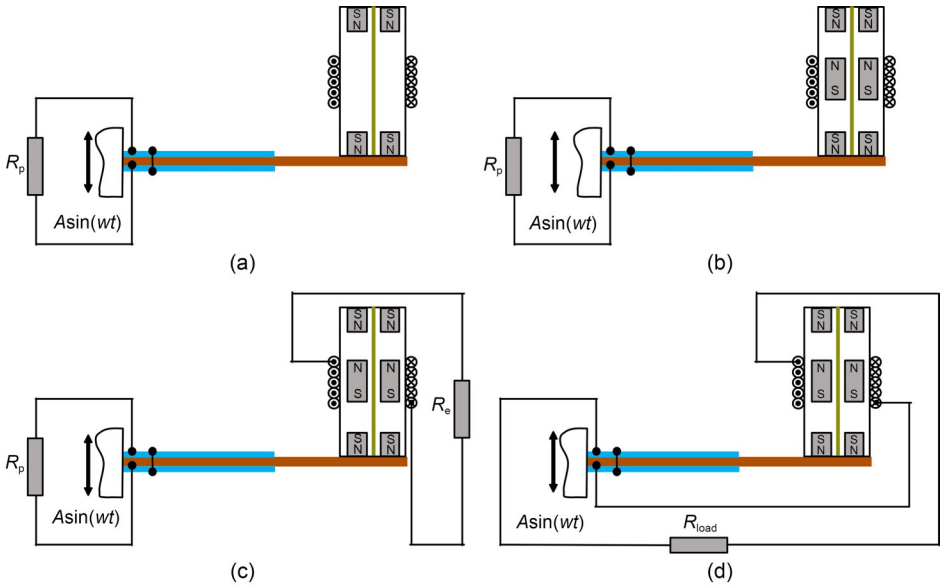

Fig. 2 Different connection topologies: (a) connection topology 1; (b) connection topology 2; (c) connection topology 3; (d) connection topology 4

R_e is connected to the induction coil. As shown in Fig. 2d, in connection topology 4 the piezoelectric and electromagnetic parts are connected electrically in series, with an extra single external load R_{load} connected. A detailed analysis of the four connection topologies is presented in the electronic supplementary materials (ESM).

4 Numerical analysis and experiments

4.1 Experimental setup

Based on the above analysis, a prototype of the studied HEHPE was prepared (as shown in the enlarged inset located in the upper right corner of Fig. 3). Related structural and material parameters are shown in Table 1. The prototype consists of a 3D-printed base made of resin materials, a 3D-printed frame made of transparent resin materials (Future Factory, China), a base beam made of red copper (Taizhou Shunkuo Hardware Products Co., Ltd., China), a ring magnet (Shanghai Strong Magnetic Material Factory, China), an induction coil, a copper bar guide, and some screws and nuts.

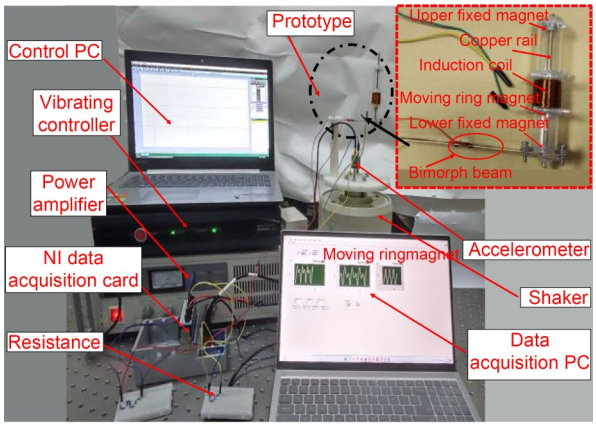

Fig. 3 Schematic diagram of the studied HEHPE (PC: personal computer; NI: National Instruments)

The main bimorph beam is composed of two PZT-5H ceramic plates (Baoding Hongsheng Electronics Co., Ltd., China) and the base beam. The two piezoelectric ceramic plates were attached to the base beam in parallel using AB glue. Both surfaces of the piezoelectric ceramic plate are covered with electrodes. The frame is attached to the free end of the base beam with the help of screws and nuts. An induction coil is wound in the middle of the frame. Two ring magnets are fixed at the upper and lower ends of the frame using solid sol. The ring magnets fixed at the upper and lower ends are connected by a thin copper rail, which guides the motion of the moving magnet.

Table 1 Parameters of the experimental prototype HEHPE

Sub structure	Parameter	Value
Base beam	Size, $L_s \times W_s \times h_s$ (mm)	63×21×0.6
	Density, ρ_s (kg/m^3)	8900
	Young's modulus, Y_s (GPa)	105
	Poisson's ratio, μ	0.324
	Extended length, L_t (mm)	31
Piezoelectric plates	Size, $L_p \times W_p \times h_p$ (mm)	40×20×0.2
	Density, ρ_p (kg/m^3)	7500
	Equivalent capacitance, C_p (nF)	110
	Piezoelectric constant, d_{31} A·s^3/(kg·m)	2.74×10^{-10}
Frame	Height×diameter (mm)	90×20
Magnets	Size of fixed ring magnet, $h \times D_o \times D_i$ (mm)	5.4×10×3
	Size of moving magnet, $h_m \times D_o \times D_i$ (mm)	12.7×10×3
	Density, ρ_m (kg/m^3)	7500
Copper rail	Height×diameter (mm)	95×2.5
Multi-turn coil	Number of turns, N	2000
	Diameter, R_c (mm)	0.01
	Thickness, h_{coil} (mm)	20
	Outer diameter, D (mm)	25
	Inner diameter, d_0 (mm)	20

W_s and h_s are the width and thickness of the base beam, respectively; W_p and h_p are the width and thickness of the piezoelectric plates, respectively; D_o and D_i are the outer diameter and inner diameter of the magnets, respectively; h and h_m are the thicknesses of fixed magnets and moving magnets, respectively

The test rig of the HEHPE is shown in Fig. 3. A vibration exciter is used to provide periodic base excitation, and its waveform and frequency are adjusted by a vibration controller, the control computer, and a power amplifier. The experimental prototype is fixed on the vibration exciter by screws. Two acceleration sensors are fixed to the base, one for detecting feedback signal and the other for monitoring the vibration controller. Voltage generated by the prototype is collected by the computer through a data acquisition card.

4.2 Comparisons of the models and the experiments

Since the lumped-parameter model described in the ESM is based on the first resonant vibration mode

of the studied HEHPE, in subsequent analysis we use only the experimental data collected for the first-order harmonic. Under different connection topologies and given external load resistance, the output voltages of the piezoelectric and electromagnetic parts, if available, are normalized with respect to the amplitude of base excitation accelerations. Results were also obtained using the lumped-parameter model with parameters tuned to match the experimental results.

For connection topologies 1 and 2, the load resistance R_p of the piezoelectric part was 70 kΩ. The resulting root-mean-square (RMS) value of the output voltage and the average power of the HEHPE were normalized (Figs. 4a and 4b, respectively). The numerical results obtained from the derived theoretical lumped-parameter models are in good agreement with the experimental results, which verifies the accuracy of the theoretical modeling. Under an excitation frequency of around 9.4 Hz, the normalized RMS voltage and average power of connection topologies 1 and 2 reached their maximums. The normalized RMS voltages per gravity acceleration amplitude were 27.84 and 24.72 for working conditions 1 and 2, respectively, while the corresponding values for the normalized average power per unit acceleration amplitude were 11.080 and 8.729, respectively. The difference is that the RMS voltage and average power of connection topology 2 showed extra peaks at a frequency of around 6.6 Hz. This is explained by the addition of a moving magnet in connection topology 2. The electromagnetic resonator thus formed interacts with the piezoelectric cantilever beam and contributes to these extra peaks.

For condition 3, the piezoelectric and electromagnetic parts of the HEHPE were electrically disconnected from each other. The external load resistance of the piezoelectric part was 70 kΩ, while that of the electromagnetic part was 150 Ω. The normalized output RMS voltage and average power of the piezoelectric part are shown in Figs. 5a and 5b, respectively, and those of the electromagnetic part in Figs. 5c and 5d, respectively.

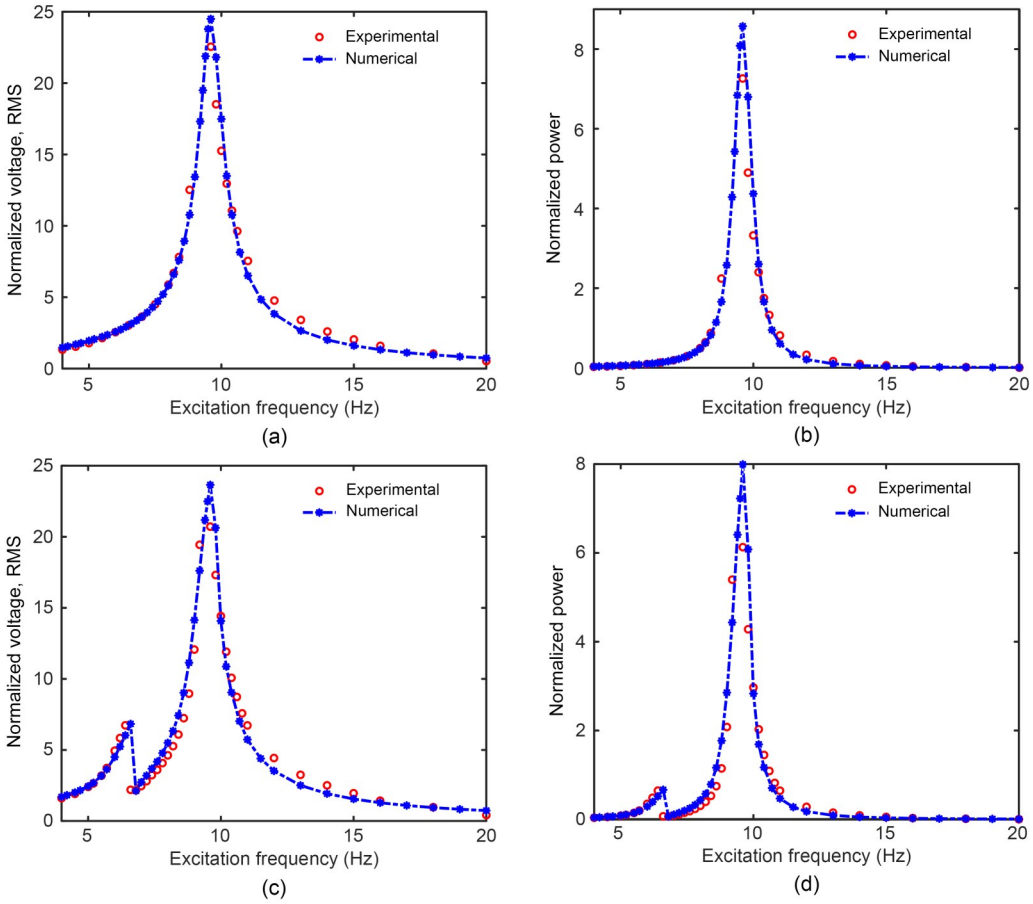

Fig. 4 Comparison of the frequency responses of RMS voltage and average power of the HEHPE obtained with different connection topologies: (a) and (b) for connection 1 and (c) and (d) for connection 2

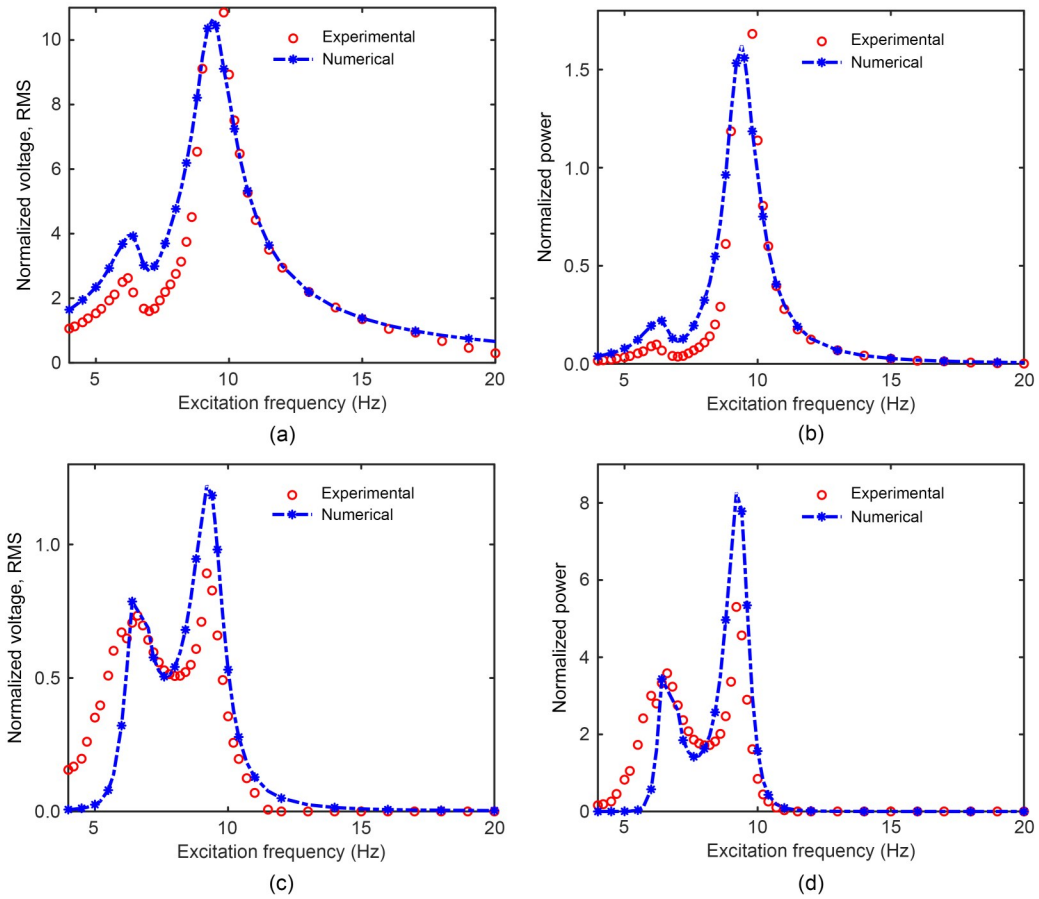

Fig. 5 Comparison of the frequency responses of RMS voltage and average power of the piezoelectric part (a and b) and electromagnetic part (c and d) obtained with connection topology 3

For both the piezoelectric and electromagnetic parts, two resonant peaks are present at the base excitation frequencies of 6.4 and 9.6 Hz, respectively. For the piezoelectric part, the normalized RMS voltages for the two resonant peaks were 2.624 and 10.850, respectively, while those for the average power were 0.91 and 1.68, respectively. For the electromagnetic part, the normalized RMS voltages for the two resonant peaks were 0.733 and 0.892, respectively, while those for average power were 3.585 and 5.300, respectively.

Comparing the results for connection topology 3 to those for connection topology 2, although the feature of two resonant peaks persists, there is an obvious decrease in the normalized RMS voltage and average power with connection topology 3. This is closely related to the addition of load resistance R_e to the electromagnetic part. In connection topology 2, the nonlinear magnetic spring is formed while no electrical output is expected without an external resistance load. No energy can be dissipated through the induction coil, and the elastic vibration of the piezoelectric part is enhanced to some degree, especially around the resonant peaks. In connection topology 3, the vibration energy of the electromagnetic part is partly dissipated through the external resistance load. As a result, energy dissipation through the external resistance load to the piezoelectric part, or the RMS voltage and average power, declined. This partly reflects the interaction between the piezoelectric and electromagnetic parts of the HEHPE. The nonlinear feature of magnetic forces is manifested in the RMS voltage and average power of the electromagnetic part (Figs. 5c and 5d, respectively). Unlike those shown in Figs. 5c and 5d, the resonant peaks for the electromagnetic part are not well separated from each other. As a consequence, the output of the electromagnetic part remains at a relatively high level for a wide range of base excitation frequencies. The average power of the electromagnetic part is essentially higher than that of the piezoelectric part. We conclude that the integration of the piezoelectric and

electromagnetic parts in an HEHPE serves to improve the working bandwidth of the system to some degree.

Note that although the experimental results obtained are in good qualitative agreement with the numerical predictions from the developed models, there are quantitative errors. One reason for this is the oversimplification of the 3D motion of the HEHPE 1D linear motion. Rotational elastic vibration of the piezoelectric cantilever beam is ignored. The swing of the electromagnetic part and revolution of the moving magnetic with respect to the copper guide rail are also neglected. A second concern is the simplified expression of the magnetic force and electromagnetic damping shown before. Moreover, although the copper guide rail was made as smooth as possible before the experiment, friction and collision between the moving magnet and the copper guide rail contribute to the differences.

To investigate the influence of the connection topology between the piezoelectric and electromagnetic parts on device performance, the two parts were electrically connected in series in connection topology 4, and a single external load resistance R_{load}=70 kΩ was adopted. The RMS output voltage and average power are shown in Figs. 6a and 6b, respectively. Resonant peaks can be seen at base excitation frequencies of 6.4 and 9.4 Hz. The RMS voltages and average powers of the HEHPE were 4.53, 14.72 and 0.3, 3.1, respectively. RMS voltages in connection topology 4 were higher than those in connection topology 3. This verifies the previous statement that mechanical interaction and electrical coupling between the piezoelectric and electromagnetic parts in the HEHPE may have a large effect on the output performance of the device.

Note that the equivalent capacitance C_p of the piezoelectric cantilever beam can be calculated as (Erturk and Inman, 2009)

$$C_p=\frac{\varepsilon_{33}^S W_p L_p}{h_p}, \tag{1}$$

where ε_{33}^S is the dielectric constant of the underlying piezoelectric material under constant strain. In this sense, the equivalent capacitance of the piezoelectric part, equivalent inductance of the electromagnetic part, and the external load R_{load} form a typical electrical oscillator circuit (Fig. 7). Combined with the equivalent inductance L_c of the induction coil, the electrical resonant frequency f_r is obtained from Eq. (2):

$$f_r=\frac{1}{2\pi\sqrt{L_c C_p}}, \tag{2}$$

where

$$L_c=\frac{7.875\times10^{-6}D_m^2N^2}{3D_m+9h_{coil}+5(D-d_0)}, \tag{3}$$

where $D_m=(D+d_0)/2$ is the average diameter of the coil.

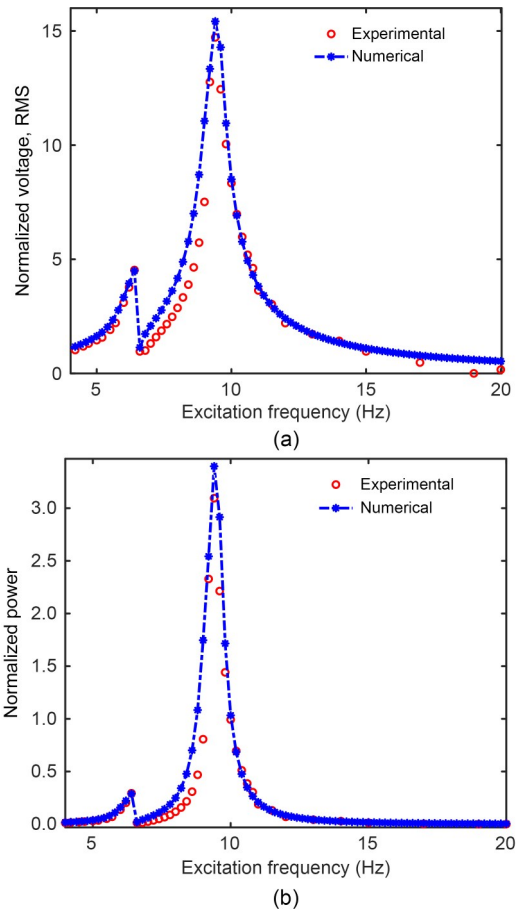

Fig. 6 Comparison of the frequency responses of RMS voltage (a) and average power (b) of the HEHPE obtained with connection topology 4

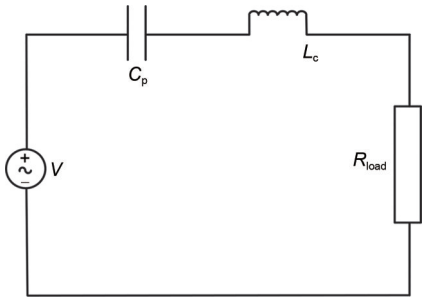

Fig. 7 Schematic diagram of the resistor-capacitor-inductor (RCL) circuit in the energy harvester device

As stated previously (Huang et al., 2022), the complex coupling between the electrical resonator, the piezoelectric part, and the electromagnetic part is seen to have the most influence on device performance. Calculations show that in our situation, the electrical resonant frequency was around 631 Hz. As this frequency is far outside the considered frequency range, the effect of the electrical resonance is not shown in our experiments. However, extra tuning of the external load circuits can help tune the output performance of HEHPEs (Huang et al., 2022). Because of the limited choice of piezoelectric and electromagnetic materials, the effect of electrical resonance has not been fully recognized. Further research is needed urgently, and this will be a topic of future investigations.

As a final characterization, considering the HEHPE in connection topology 3, different external load resistances were applied to the piezoelectric part (1–1000 kΩ) and electromagnetic part (10–5000 Ω), respectively. The RMS voltage and average power of the HEHPE are shown in Fig. 8. With increasing load resistance, the output voltage amplitude gradually increases, and finally approaches a limit (Figs. 8a and 8c). The average output power first reaches the maximum value at the optimal load, and then decreases monotonically with the further increase of load resistance (Figs. 8b and 8d). The predictions from our lumped-parameter models are also shown.

Note that when the base excitation frequency is far from the resonant frequencies (here we aimed for a resonant frequency of around 6.4 Hz), the numerical predictions are in good agreement with the experiment results. However, when the base excitation frequency is close to the resonance, numerical predictions deviate from experimental results. This is consistent with our model assumption that the electromagnetic and piezoelectric parts weakly interact with each other. Close to resonance, however, the interaction between

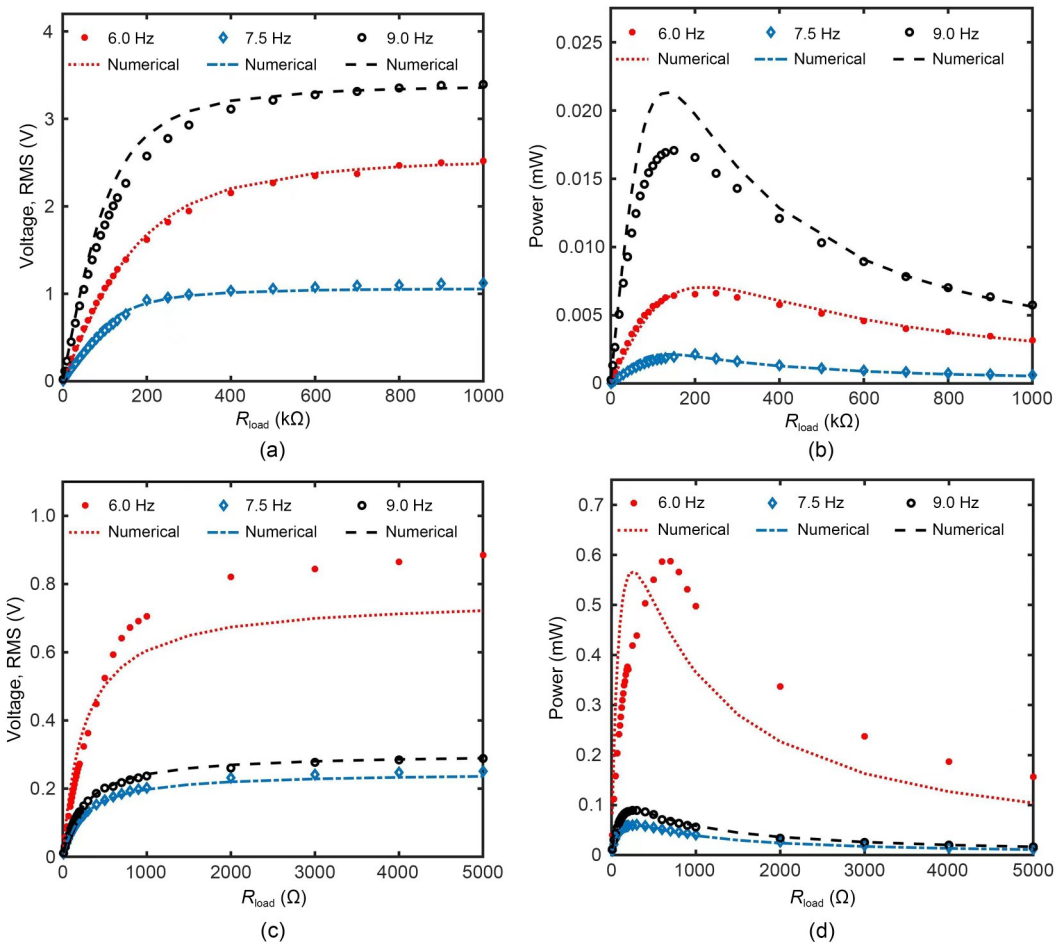

Fig. 8 Outputs of the HEHPE with connection topology 3 at excitation frequencies of 6.0, 7.5, and 9.0 Hz: RMS voltage (a) and average power (b) for the piezoelectric part; RMS voltage (c) and average power (d) for the electromagnetic part

these two parts is strong with dramatic energy exchange, which is not accounted for in the simplified model. Nonlinearity and mutual coupling in the HEHPE need extra attention in future investigations.

4.3 Modifications of the electromagnetic part

Results from previous experiments gave us the impression that a moving magnet in the electromagnetic part does not move far from its balanced position. As a consequence, the RMS output voltage of the electromagnetic part shown in Fig. 8 is far from satisfactory. A direct cause is that the magnetic force is too strong for the moving magnet to move easily. To strengthen the motion of the moving magnet, we replaced the upper fixed magnet in the electromagnetic part with an elastic spring. A schematic diagram of the modified system is shown in Fig. 9. The main idea is that when the moving magnet oscillates, it will collide with the elastic spring. Non-smooth nonlinearity is introduced into the system and the oscillating amplitude of the moving magnet can be increased (Xu et al., 2017a).

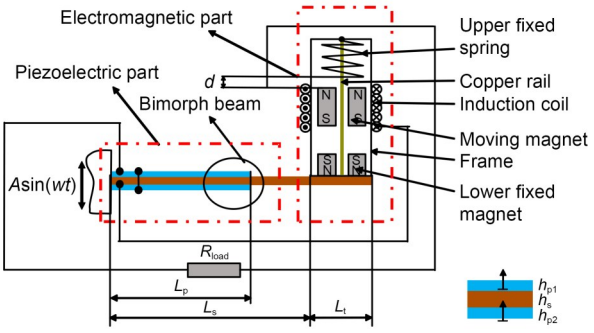

Fig. 9 Diagram of the structure of the modified HEHPE with the upper fixed magnet replaced with a fixed spring

To begin with, we were concerned about the distance d between the elastic spring and the moving magnet (Fig. 9). Its influence upon device performance was explored. The values of d were set to 0, 2, and 4 mm, respectively. Under connection topology 3, the RMS voltages of the piezoelectric part and the electromagnetic part were as shown in Figs. 10a and 10b, respectively, versus the base excitation frequency. Under connection topology 4, the RMS voltage of the HEHPE was as shown in Fig. 11.

In Figs. 10a and 11, with increasing d, the RMS voltage for the first resonant peak decreases gradually, while that for the second peak increases, while in Fig. 10b, the RMS voltage of both resonant peaks decreases with increasing d and gradually approachs

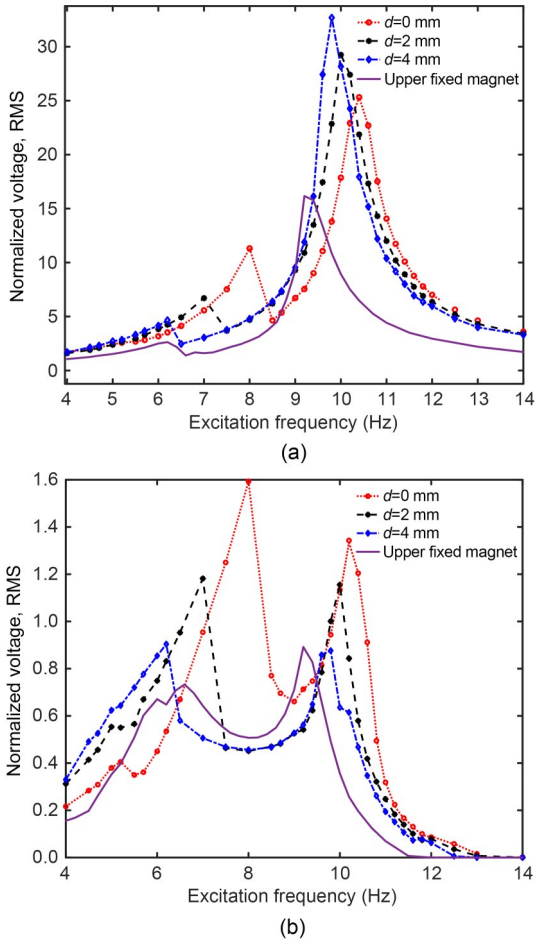

Fig. 10 Output performance of the modified HEHPE with different d with connection topology 3: (a) RMS voltage of the piezoelectric part; (b) RMS voltage of the electromagnetic part

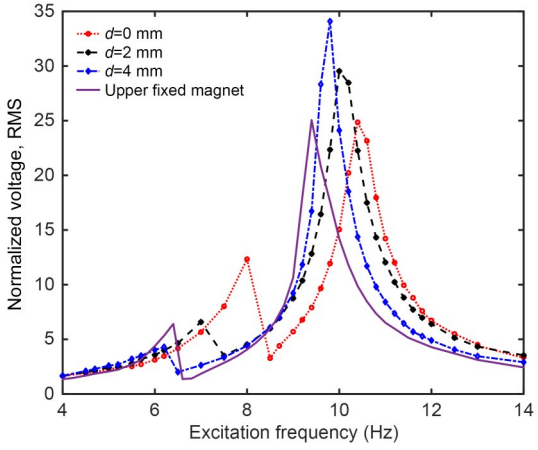

Fig. 11 Output voltage of the modified HEHPE with different d with connection topology 4

that of the original HEHPE prototype. Note that replacement of the upper fixed magnet with an elastic spring increased the output performance of the device for nearly all connection topologies. Besides, due to the introduction of collision between the moving magnet and the elastic spring, up-conversion of the frequency is apparent in Figs. 10 and 11.

Since the mathematical model of the modified HEHPE is not well established, detailed discussions are postponed. In future investigations, a search for an optimal value of d could be of primary interest to improve device performance. In addition, the stiffness of the elastic spring was not carefully tuned in our small-scale experiments. Future investigations should be done to elucidate its effects.

5 Conclusions

With increasing attention being paid to PVEHs, researchers are attempting to increase their working bandwidths through the integration of piezoelectric and electromagnetic energy transduction mechanisms in a single HEHPE.

This study focused on the nonlinear interaction in an HEHPE. Mathematical models of the proposed HEHPE were established considering different connection topologies. Prototypes were prepared and tested. Input and output signals of the HEHPE were firstly analyzed to stress the insufficiently understood features of containing multi-frequency components. Methods for characterizing such signals are put forward and discussed. With regard to different connection topologies, the RMS voltage and average power of the HEHPE were investigated and compared with numerical predictions based on a developed model. Good agreement was found. We also found that the electrical connection between the electromagnetic and piezoelectric parts in the HEHPE serves to tune the frequency characteristics of the device and alter its output performance. Nonlinearity due to the magnetic force introduced also changes the energy distribution between the electromagnetic and piezoelectric parts. Once system parameters are well tuned, better device performance in terms of working bandwidth and output power can be expected.

Also, the original HEHPE was modified by replacing the upper fixed magnet with an elastic spring. An obvious performance improvement was witnessed and considerable frequency tuning observed. Changing the distance d between the spring and the moving magnet was shown to greatly affect device behavior.

Nonetheless, several points need attention in future research. The base beam in the piezoelectric part should be longer and thicker, to make it easier to match the resonant properties of the piezoelectric and electromagnetic parts. Besides, tuning of the resonant frequency due to the electrical connection between the piezoelectric part and the electromagnetic should be optimized. In addition, a detailed study of the modified HEHPE is needed to provide a thorough understanding of the effect of the introduced nonlinearity on device performance.

Acknowledgments

This work is supported by the Zhejiang Provincial Natural Science Foundation of China (No. LY22E050013) and the China Postdoctoral Science Foundation (No. 2021M690545), and is also supported in part by the Zhejiang Provincial Natural Science Foundation of China (No. LZY22E050001) and the National Natural Science Foundation of China (No. 51805124).

Author contributions

Shifan HUANG, Zhenlong XU, and Maoying ZHOU designed the research. Shifan HUANG and Weihao LUO processed the corresponding data. Shifan HUANG wrote the first draft of the manuscript. Weihao LUO, Zongming ZHU, Ban WANG, and Huawei QIN helped to organize the manuscript. Maoying ZHOU and Shifan HUANG revised and edited the final version.

Conflict of interest

Shifan HUANG, Weihao LUO, Zongming ZHU, Zhenlong XU, Ban WANG, Maoying ZHOU, and Huawei QIN declare that they have no conflict of interest.

References

Ahmad MM, Khan FU, 2021. Review of vibration-based electromagnetic–piezoelectric hybrid energy harvesters. *International Journal of Energy Research*, 45(4):5058-5097. https://doi.org/10.1002/er.6253

Anton SR, Sodano HA, 2007. A review of power harvesting using piezoelectric materials (2003-2006). *Smart Materials and Structures*, 16(3):R1-R21. https://doi.org/10.1088/0964-1726/16/3/r01

Arroyo E, Badel A, Formosa F, et al., 2012. Comparison of electromagnetic and piezoelectric vibration energy harvesters: model and experiments. *Sensors and Actuators A: Physical*, 183:148-156. https://doi.org/10.1016/j.sna.2012.04.033

Basset P, Galayko D, Cottone F, et al., 2014. Electrostatic vibration energy harvester with combined effect of electrical nonlinearities and mechanical impact. *Journal of Micromechanics and Microengineering*, 24(3):035001. https://doi.org/10.1088/0960-1317/24/3/035001

Cao DX, Leadenham S, Erturk A, 2015. Internal resonance for nonlinear vibration energy harvesting. *The European Physical Journal Special Topics*, 224(14-15):2867-2880. https://doi.org/10.1140/epjst/e2015-02594-4

Challa VR, Prasad MG, Fisher FT, 2009. A coupled piezoelectric–electromagnetic energy harvesting technique for achieving increased power output through damping matching. *Smart Materials and Structures*, 18(9):095029. https://doi.org/10.1088/0964-1726/18/9/095029

Challa VR, Prasad MG, Fisher FT, 2011. Towards an autonomous self-tuning vibration energy harvesting device for wireless sensor network applications. *Smart Materials and Structures*, 20(2):025004. https://doi.org/10.1088/0964-1726/20/2/025004

Dechant E, Fedulov F, Fetisov LY, et al., 2017. Bandwidth widening of piezoelectric cantilever beam arrays by mass-tip tuning for low-frequency vibration energy harvesting. *Applied Sciences*, 7(12):1324. https://doi.org/10.3390/app7121324

Erturk A, Inman DJ, 2009. An experimentally validated bimorph cantilever model for piezoelectric energy harvesting from base excitations. *Smart Materials and Structures*, 18(2): 025009. https://doi.org/10.1088/0964-1726/18/2/025009

Fan KQ, Tan QX, Liu HY, et al., 2018a. Hybrid piezoelectric-electromagnetic energy harvester for scavenging energy from low-frequency excitations. *Smart Materials and Structures*, 27(8):085001. https://doi.org/10.1088/1361-665X/aaae92

Fan KQ, Tan QX, Zhang YW, et al., 2018b. A monostable piezoelectric energy harvester for broadband low-level excitations. *Applied Physics Letters*, 112(12):123901. https://doi.org/10.1063/1.5022599

Fan KQ, Liu SH, Liu HY, et al., 2018c. Scavenging energy from ultra-low frequency mechanical excitations through a bi-directional hybrid energy harvester. *Applied Energy*, 216:8-20. https://doi.org/10.1016/j.apenergy.2018.02.086

Halim MA, Kabir MH, Cho H, et al., 2019. A frequency up-converted hybrid energy harvester using transverse impact-driven piezoelectric bimorph for human-limb motion. *Micromachines*, 10(10):701. https://doi.org/10.3390/mi10100701

Huang SF, Zhou MY, Liu Y, 2022. Output performance of piezoelectric vibration energy harvester considering inductive loads. Proceedings of the Eighth Asia International Symposium on Mechatronics, p.167-172. https://doi.org/10.1007/978-981-19-1309-9_16

Iqbal M, Nauman MM, Khan FU, et al., 2021. Vibration-based piezoelectric, electromagnetic, and hybrid energy harvesters for microsystems applications: a contributed review. *International Journal of Energy Research*, 45(1):65-102. https://doi.org/10.1002/er.5643

Kandris D, Nakas C, Vomvas D, et al., 2020. Applications of wireless sensor networks: an up-to-date survey. *Applied System Innovation*, 3(1):14. https://doi.org/10.3390/asi3010014

Li P, Gao SQ, Cai HT, et al., 2016. Theoretical analysis and experimental study for nonlinear hybrid piezoelectric and electromagnetic energy harvester. *Microsystem Technologies*, 22(4):727-739. https://doi.org/10.1007/s00542-015-2440-8

Li YF, Cheng G, Lin ZH, et al., 2015. Single-electrode-based rotationary triboelectric nanogenerator and its applications as self-powered contact area and eccentric angle sensors. *Nano Energy*, 11:323-332. https://doi.org/10.1016/j.nanoen.2014.11.010

Liu HC, Fu HL, Sun LN, et al., 2021. Hybrid energy harvesting technology: from materials, structural design, system integration to applications. *Renewable and Sustainable Energy Reviews*, 137:110473. https://doi.org/10.1016/j.rser.2020.110473

Liu HP, Gao SQ, Wu JR, et al., 2019. Study on the output performance of a nonlinear hybrid piezoelectric-electromagnetic harvester under harmonic excitation. *Acoustics*, 1(2):382-392. https://doi.org/10.3390/acoustics1020021

Maamer B, Boughamoura A, Fath El-Bab AMR, et al., 2019. A review on design improvements and techniques for mechanical energy harvesting using piezoelectric and electromagnetic schemes. *Energy Conversion and Management*, 199:111973. https://doi.org/10.1016/j.enconman.2019.111973

Mahmoudi S, Kacem N, Bouhaddi N, 2014. Enhancement of the performance of a hybrid nonlinear vibration energy harvester based on piezoelectric and electromagnetic transductions. *Smart Materials and Structures*, 23(7):075024. https://doi.org/10.1088/0964-1726/23/7/075024

Malik BT, Doychinov V, Hayajneh AM, et al., 2020. Wireless power transfer system for battery-less sensor nodes. *IEEE Access*, 8:95878-95887. https://doi.org/10.1109/access.2020.2995783

Miller T, Oyewobi SS, Abu-Mahfouz AM, et al., 2020. Enabling a battery-less sensor node using dedicated radio frequency energy harvesting for complete off-grid applications. *Energies*, 13(20):5402. https://doi.org/10.3390/en13205402

Priyadarshi R, Gupta B, Anurag A, 2020. Deployment techniques in wireless sensor networks: a survey, classification, challenges, and future research issues. *The Journal of Supercomputing*, 76(9):7333-7373. https://doi.org/10.1007/s11227-020-03166-5

Qiu CK, Wu F, Lee C, et al., 2020. Self-powered control interface based on gray code with hybrid triboelectric and photovoltaics energy harvesting for IoT smart home and access control applications. *Nano Energy*, 70:104456. https://doi.org/10.1016/j.nanoen.2020.104456

Safaei M, Sodano HA, Anton SR, 2019. A review of energy harvesting using piezoelectric materials: state-of-the-art a decade later (2008-2018). *Smart Materials and Structures*, 28(11):113001.

https://doi.org/10.1088/1361-665X/ab36e4

Sang YJ, Huang XL, Liu HX, et al., 2012. A vibration-based hybrid energy harvester for wireless sensor systems. *IEEE Transactions on Magnetics*, 48(11):4495-4498. https://doi.org/10.1109/tmag.2012.2201452

Saravia CM, 2019. A formulation for modeling levitation based vibration energy harvesters undergoing finite motion. *Mechanical Systems and Signal Processing*, 117:862-878. https://doi.org/10.1016/j.ymssp.2018.08.023

Shan XB, Guan SW, Liu ZS, et al., 2013. A new energy harvester using a piezoelectric and suspension electromagnetic mechanism. *Journal of Zhejiang University-SCIENCE A (Applied Physics & Engineering)*, 14(12):890-897. https://doi.org/10.1631/jzus.A1300210

Shi G, Chen JF, Peng YS, et al., 2020. A piezo-electromagnetic coupling multi-directional vibration energy harvester based on frequency up-conversion technique. *Micromachines*, 11(1):80. https://doi.org/10.3390/mi11010080

Tran N, Ghayesh MH, Arjomandi M, 2018. Ambient vibration energy harvesters: a review on nonlinear techniques for performance enhancement. *International Journal of Engineering Science*, 127:162-185. https://doi.org/10.1016/j.ijengsci.2018.02.003

Wang B, Zhou MY, Zhu DF, et al., 2022. Modeling and analysis of the piezoelectric vibration energy harvester with externally connected inductor. *Acta Mechanica*, 233(7): 2701-2717. https://doi.org/10.1007/s00707-022-03248-w

Wang W, Wei HT, Wei ZH, 2022. Numerical analysis of a magnetic-spring-based piecewise nonlinear electromagnetic energy harvester. *The European Physical Journal Plus*, 137(1):56. https://doi.org/10.1140/epjp/s13360-021-02255-5

Wang ZM, Du Y, Li TR, et al., 2022. Bioinspired omnidirectional piezoelectric energy harvester with autonomous direction regulation by hovering vibrational stabilization. *Energy Conversion and Management*, 261:115638. https://doi.org/10.1016/j.enconman.2022.115638

Wu ZH, Xu QS, 2022. Design of a structure-based bistable piezoelectric energy harvester for scavenging vibration energy in gravity direction. *Mechanical Systems and Signal Processing*, 162:108043. https://doi.org/10.1016/j.ymssp.2021.108043

Xia HK, Chen RW, Ren L, 2015. Analysis of piezoelectric–electromagnetic hybrid vibration energy harvester under different electrical boundary conditions. *Sensors and Actuators A: Physical*, 234:87-98. https://doi.org/10.1016/j.sna.2015.08.014

Xia HK, Chen RW, Ren L, 2017. Parameter tuning of piezoelectric–electromagnetic hybrid vibration energy harvester by magnetic force: modeling and experiment. *Sensors and Actuators A: Physical*, 257:73-83. https://doi.org/10.1016/j.sna.2017.01.026

Xu ZL, Shan XB, Chen DP, et al., 2016. A novel tunable multi-frequency hybrid vibration energy harvester using piezoelectric and electromagnetic conversion mechanisms. *Applied Sciences*, 6(1):10. https://doi.org/10.3390/app6010010

Xu ZL, Wang W, Xie J, et al., 2017a. An impact-based frequency up-converting hybrid vibration energy harvester for low frequency application. *Energies*, 10(11):1761. https://doi.org/10.3390/en10111761

Xu ZL, Shan XB, Yang H, et al., 2017b. Parametric analysis and experimental verification of a hybrid vibration energy harvester combining piezoelectric and electromagnetic mechanisms. *Micromachines*, 8(6):189. https://doi.org/10.3390/mi8060189

Yang B, Lee C, Kee WL, et al., 2010. Hybrid energy harvester based on piezoelectric and electromagnetic mechanisms. *Journal of Micro/Nanolithography*, 9(2):023002. https://doi.org/10.1117/1.3373516

Yao BK, Gao H, Zhang Y, et al., 2023. Maximum AoI minimization for target monitoring in battery-free wireless sensor networks. *IEEE Transactions on Mobile Computing*, 22(8):4754-4772. https://doi.org/10.1109/TMC.2022.3161975

Zhang GY, Gao SQ, Liu HP, et al., 2019. Design and performance of hybrid piezoelectric-electromagnetic energy harvester with trapezoidal beam and magnet sleeve. *Journal of Applied Physics*, 125(8):084101. https://doi.org/10.1063/1.5087024

Zhang JH, Qin LF, 2019. A tunable frequency up-conversion wideband piezoelectric vibration energy harvester for low-frequency variable environment using a novel impact- and rope-driven hybrid mechanism. *Applied Energy*, 240:26-34. https://doi.org/10.1016/j.apenergy.2019.01.261

Zhang Y, Cai CS, Kong B, 2015. A low frequency nonlinear energy harvester with large bandwidth utilizing magnet levitation. *Smart Materials and Structures*, 24(4):045019. https://doi.org/10.1088/0964-1726/24/4/045019

Zhang YL, Wang TY, Zhang A, et al., 2016. Electrostatic energy harvesting device with dual resonant structure for wideband random vibration sources at low frequency. *Review of Scientific Instruments*, 87(12):125001. https://doi.org/10.1063/1.4968811

Zhang YL, Wang TY, Luo AX, et al., 2018. Micro electrostatic energy harvester with both broad bandwidth and high normalized power density. *Applied Energy*, 212:362-371. https://doi.org/10.1016/j.apenergy.2017.12.053

Zhou MY, Al-Furjan MSH, Zou J, et al., 2018. A review on heat and mechanical energy harvesting from human–principles, prototypes and perspectives. *Renewable and Sustainable Energy Reviews*, 82:3582-3609. https://doi.org/10.1016/j.rser.2017.10.102

Zhu G, Lin ZH, Jing QS, et al., 2013. Toward large-scale energy harvesting by a nanoparticle-enhanced triboelectric nanogenerator. *Nano Letters*, 13(2):847-853. https://doi.org/10.1021/nl4001053

Zou HX, Zhang WM, Li WB, et al., 2017. Design and experimental investigation of a magnetically coupled vibration energy harvester using two inverted piezoelectric cantilever beams for rotational motion. *Energy Conversion and Management*, 148:1391-1398. https://doi.org/10.1016/j.enconman.2017.07.005

Electronic supplementary materials

Sections S1 and S2